Quantitative Imaging of Ozone Vapor Using Photofragmentation Laser-Induced Fluorescence (LIF)

Larsson, Kajsa; Hot, Dina; Ehn, Andreas; Lantz, Andreas; Weng, Wubin; Aldén, Marcus; Bood, Joakim

Published in:
Applied Spectroscopy

DOI:
10.1177/0003702817691528

2017

Document Version:
Publisher's PDF, also known as Version of record

Article

Applied Spectroscopy

Applied Spectroscopy
2017, Vol. 71(7) 1578–1585

DOI: 10.1177/0003702817691528
journals.sagepub.com/home/asp
SAGE

Quantitative Imaging of Ozone Vapor Using Photofragmentation Laser-Induced Fluorescence (LIF)

Kajsa Larsson[1], Dina Hot[1], Andreas Ehn[1], Andreas Lantz[1,2], Wubin Weng[1], Marcus Aldén[1], and Joakim Bood[1]

Abstract

In the present work, the spectral properties of gaseous ozone (O_3) have been investigated aiming to perform quantitative concentration imaging of ozone by using a single laser pulse at 248 nm from a KrF excimer laser. The O_3 molecule is first photodissociated by the laser pulse into two fragments, O and O_2. Then the same laser pulse electronically excites the O_2 fragment, which is vibrationally hot, whereupon fluorescence is emitted. The fluorescence intensity is found to be proportional to the concentration of ozone. Both emission and absorption characteristics have been investigated, as well as how the laser fluence affects the fluorescence signal. Quantitative ozone imaging data have been achieved based on calibration measurements in known mixtures of O_3. In addition, a simultaneous study of the emission intensity captured by an intensified charge-coupled device (ICCD) camera and a spectrograph has been performed. The results show that any signal contribution not stemming from ozone is negligible compared to the strong fluorescence induced by the O_2 fragment, thus proving interference-free ozone imaging. The single-shot detection limit has been estimated to ~400 ppm. The authors believe that the presented technique offers a valuable tool applicable in various research fields, such as plasma sterilization, water and soil remediation, and plasma-assisted combustion.

Keywords

Ozone, photofragmentation, laser-induced fluorescence, LIF, imaging

Date received: 12 September 2016; accepted: 6 December 2016

Introduction

Most of the ozone (O_3) present on earth is found in the stratosphere, where it is paramount for absorption of ultraviolet (UV) radiation emitted by the sun.[1] It is formed by UV (< 240 nm) photolysis of O_2 into oxygen atoms, which reform into O_3 by reacting with O_2. Extensive research efforts have been carried out on ozone in the atmosphere, see Seinfeld and Pandis[1] and Kondratyev and Varotsos.[2]

Besides its vital role in atmospheric chemistry, ozone is also of great importance in several technical applications, for example plasma-assisted combustion (PAC) and the food packaging industry. The main idea with PAC is to add a relatively small amount of electronic energy to a flame to gain a large effect on the combustion chemistry. Ozone is one species among others that may be added to a flame to increase the electric energy, others are, for example, free electrons and oxygen ions.[3–5] Ozone is a rather long-lived species, wherefore it is easier to inject compared to short-lived species like free electrons and radicals. Liang et al.[6] have listed some experimental studies of ozone injection in flames. These authors have also investigated how the laminar burning velocity is affected by ozone addition (2500–8000 ppm) to H_2–CO–N_2–air premixed flames at ambient conditions, and they found that the laminar burning velocity was enhanced both for rich and lean mixtures when ozone was injected.

Further, in sterilization processes, where the aim is to eliminate microbial contamination, non-thermal atmospheric plasmas have gained interest in the last couple of years. Microbial reactive species like O_3 and NO_2 are created in a plasma discharge[7] and detection of these species is therefore crucial in order to understand the microbial

[1]Division of Combustion Physics, Lund University, Lund, Sweden
[2]Current address: Siemens Industrial Turbomachinery AB, Finspång, Sweden

Corresponding author:
Dina Hot, Division of Combustion Physics, Lund University, P.O. Box 118, 221 00 Lund, Sweden.
Email: dina.hot@forbrf.lth.se

deactivation process. Laroussi et al.[8] present an overview of how different parameters in plasma-based sterilization, such as heat, reactive species, and charged particles, affect cells in microorganisms. In that work,[8] the ozone concentration in the plasma was measured using absorption spectroscopy and it was found that the ozone concentration was on the order of 2000 ppm. For more details concerning plasma sterilization the reader is referred to the references.[9–12]

Because of the strong oxidizing effect of ozone it may be used for remediation of contaminated substances, e.g., soil and water. Oil and fuel spill from cars and trucks is a worldwide problem that causes soils contaminated by polycyclic aromatic hydrocarbons (PAH). For in situ remediation of PAH-contaminated soil, injected ozone gas is one of the most promising techniques since it can either directly react with organic/inorganic contaminants or decompose into OH radicals, which in turn can react with unwanted species in the soil.[13–16] Moreover, ozone may also be directly injected into water to ensure disinfection of for example drinking water. For more details about water remediation processes the reader is referred to the references.[17,18]

The absorption spectrum of ozone consists of three bands, the Hartley band, the Huggins band, and the Chappius band. The Hartley band peaks at roughly 260 nm, while the Huggins band is in the range of 310–360 nm at the long wavelength tail of the Hartley band. The Chappius band, on the other hand, has its maximum absorption in the visible region around 600 nm[1]. An example where the absorption features of the Hartley band is used for diagnostic purposes was presented by Ono and Oda.[19] They measured the density of ozone in a pulsed corona discharge by determining the laser absorption with a KrF excimer laser.

Laser-induced fluorescence (LIF) is a mature diagnostic technique that has been widely applied for flow visualization of liquid, gas, and plasma. It has the capability of measuring species-specific trace concentrations with high temporal and spatial resolution, and is utilized in many different research fields and applications. Two-dimensional (2D) imaging, allowing for example snapshots of flow structures in turbulent environments, can be achieved by turning the laser beam into a laser sheet, which is commonly referred to as planar laser-induced fluorescence (PLIF). Theory, concepts, and examples of applications for gas-phase diagnostics with LIF have been described in review articles by Kohse-Höinghaus,[20] Daily,[21] and Aldén et al.[22] The ozone molecule is, however, dissociated when illuminated with laser radiation below 1180 nm,[23] preventing direct detection with LIF in the UV-Vis (Vis)/near-infrared (NIR) spectral regions. Nevertheless, it is possible to detect ozone by first photodissociating the molecule with a pump photon, creating O and O_2, whereupon a second photon (probe) detects the O_2 photofragment using PLIF. This pump–probe technique is called photofragmentation laser induced fluorescence (PF-LIF) and has previously been applied for visualization of hydrogen peroxides in free gas flows,[24,25] flames,[26] and combustion engines.[27] Furthermore, Pitz et al. have previously applied the measurement concept in flow-field velocimetry based on photochemical ozone production.[28]

In the present work, PF-LIF imaging of ozone based on a single KrF laser pulse at 248 nm is carried out. The spectroscopic characteristics, i.e., excitation and emission spectra, are thoroughly investigated and the signal strengths for imaging and spectrally resolved measurements are compared, before quantitative 2D imaging is demonstrated and discussed.

Measurement Concept

Photofragmentation laser-induced fluorescence is a measurement concept that can be utilized for 2D visualization of species that lack bound excited electronic transitions. Ozone is such a species and PF-LIF, based on a KrF excimer laser, was therefore applied in this work. A schematic illustration of PF-LIF for O_3 detection is presented in Figure 1. First, a pump photon is used to photodissociate the O_3 molecule into a vibrationally excited O_2 molecule and an electronically excited oxygen atom. Second, a probe photon is used to electronically excite the vibrationally excited O_2 molecule, which after relaxation either emits fluorescence or dissociates into oxygen atoms (each in the electronic ground state). Having the KrF excimer laser tuned to an absorption line of the vibrationally excited O_2 thus allows pumping and probing with the same laser pulse.

Photofragmentation of ozone in the UV leads to several different energy level distributions of the photofragments, where the main dissociation channels are $O_2(\alpha^1\Delta_g) + O(^1D)(>90\%)$ and $O_2(X^3\Sigma_g^-) + O(^3P)$. The

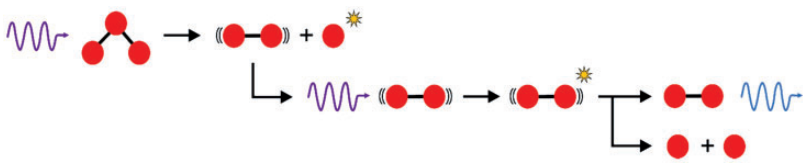

Figure 1. Schematic of the PF-LIF of O_3.

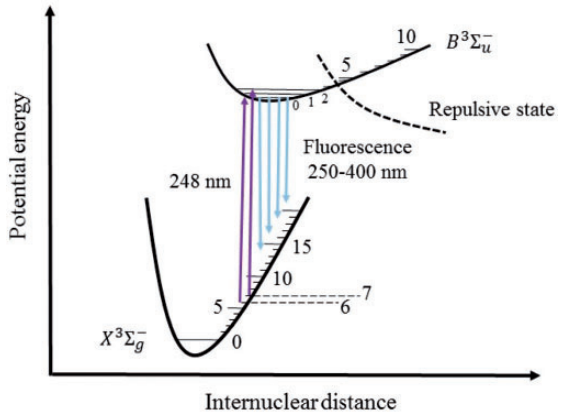

Figure 2. Schematic energy level diagram of the involved O_2 LIF transitions. Adapted from Grinstead et al.[29]

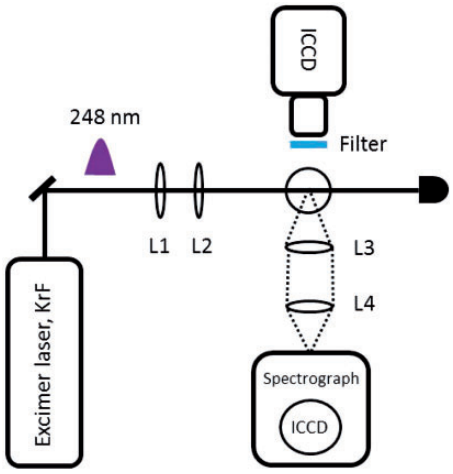

Figure 3. Schematic illustration of the experimental setup. A tunable KrF excimer laser was used as light source. Lenses L1 and L2 are laser sheet-forming optics and L3 and L4 are collecting optics for the spectrograph. Ozone concentrations in the range of 0.1–5% were used in the measurement volume.

measurement concept presented in this work is based on LIF from the $O_2(X^3\Sigma_g^-)$ fragment.[23] The O (^1D), which is the major product channel for O-atoms, is aggressive and reacts rapidly with, e.g., H_2O or CH_4. Such effects should be considered if multiple species are being measured simultaneously since the 248 nm pulse could alter the chemical condition on short time scales. In addition, effect on the overall chemistry might occur if lasers with high repetition rates are used. An energy level diagram of the transitions involved in the LIF process of O_2 is presented in Figure 2. The high energy of the 248 nm pump photon creates vibrationally hot O_2 photofragments. The probe photon, whose energy matches the transitions indicated by the purple arrows in Figure 2, excites the vibrationally hot O_2 photofragments present in the $X^3\Sigma_g^-$, v''=6,7 states to the $B^3\Sigma_u^-$, $v' = 0,2$ states, corresponding to the wavelength range of 248–248.8 nm. Oxygen molecules naturally present in the ambient air are in thermal equilibrium and thus only populate the vibrational ground state and will not be excited by the probe pulse since the energy difference between the ground and the excited state is larger than the energy of a 248 nm photon. Thus, all detected O_2 fluorescence comes from O_2 photofragments stemming from photolysis of O_3. The dominant loss mechanism in the $B^3\Sigma_u^-$ states is predissociation as the molecules transfers to the nearby repulsive state. However, a small fraction of the excited O_2 photofragments emits fluorescence in the range of 250–450 nm, as indicated by the light blue arrows in Figure 2.

Experimental

A schematic of the experimental setup is shown in Figure 3. It consisted of a KrF excimer laser (LambdaPhysik, EMG-150 MSC), optical components (mirrors, lenses, and filters), an ozone generator (O3-Technology, AC-20), and two different arrangements for signal detection. The excimer laser is tunable from 247.9 nm to 248.9 nm and operated at a pulse repetition rate of 10 Hz, producing pulses of ~17 ns duration and 100 mJ energy with a line width of 0.2 cm^{-1} (full width half maximum (FWHM)). First, the laser beam propagated through sheet-forming optics to obtain a rectangular beam profile. The sheet-forming optics consisted of two cylindrical lenses; one with focal length $f = 400$ mm (L1), focusing in the vertical direction, and one with $f = 200$ mm (L2), focusing in the horizontal direction. The laser beam then propagated through the measurement volume, containing an ozone gas flow, before it terminated in a beam dump. The detection systems for the O_2 fluorescence consisted of an intensified CCD camera (Princeton Instruments, PI-MAX 2) equipped with a UV-Nikkor lens ($f = 105$ mm, f/4.5) during the 2D imaging measurements, while a 0.5 m focal length spectrograph (Princeton Instruments, Acton Series SP 2556) connected to an ICCD camera (Princeton Instruments, PI-MAX 3) was employed during the spectroscopic investigations. A liquid *n*-butyl acetate filter was placed in front of the camera in order to suppress scattered laser radiation while the grating of the spectrograph was positioned for analysis of emission above 260 nm. Two spherical lenses with focal lengths $f = 150$ mm (L3) and $f = 200$ mm (L4) were placed in front of the spectrograph in order to collect the fluorescence signal and focus it onto the entrance slit of the spectrograph.

The ozone in the measurement volume was generated by supplying oxygen through the ozone generator. The oxygen gas flow was controlled using calibrated mass flow controllers (Bronkhorst). By varying the flow of oxygen as well as the conversion efficiency of the ozone generator, it was possible to change the concentration of ozone in the measurement volume. Ozone concentrations in the range

of 0.1–5% (diluted in oxygen) were used in this work. In addition, ozone was measured in a CH_4/air/O_3 gas mixing reactor configuration. The gas mixtures were preheated in the mixing process to initiate thermal decomposition of O_3, which thus changed the concentration of ozone. The emission signals were captured both with the imaging CCD camera and the spectrograph setup to ensure that the technique could be used for imaging of O_3 while methane is present in the gas mixture. An equivalence ratio of 0.65 was kept throughout these measurements.

Results and Discussion

Spectroscopic Investigation

A spectroscopic investigation of the O_2 fluorescence was performed by simultaneously recording excitation and emission spectra. Such spectroscopic information was achieved by scanning the excimer laser wavelength between 247.9 and 248.9 nm while flowing ozone gas in the measurement volume and detecting the emission through the spectrograph. In Figure 4a, the recorded data have been synthesized into a 2D map with excitation wavelength on the ordinate and emission wavelength on the abscissa. Figure 4b shows an excitation spectrum corresponding to a horizontal integration of the signal indicated by the dashed vertical box in Figure 4a, which is associated with the emission line (0–13). Figure 4c displays an emission spectrum corresponding to a vertical integration of the signal in the dashed horizontal box in Figure 4a, which is obtained by scanning the laser wavelength over the closely spaced absorption lines P(13) (0–6) and R(11) (2–7). The absorption lines in Figure 4b agree well with the absorption lines in the work of Andresen et al.[30] The majority of the fluorescence signal originates from the $v' = 0 \leftarrow v'' = 6$ transition with a small contribution from the $v' = 2 \leftarrow v'' = 7$ transition. The dispersed emission spectrum shown in Figure 4c agrees well with spectra reported by Grinstead et al.,[29] showing that the detected signal indeed is fluorescence from vibrationally hot O_2 stemming from dissociation of O_3.

The O_2 fluorescence signal intensity was investigated for different known ozone concentrations and the result is summarized in the graph shown in Figure 5. The uncertainty in the ozone concentration is mainly due to the uncertainty in the mass flow controllers and was found to be approximately ± 2.6 % of the ozone concentration. The O_2 LIF data points follow a straight line corresponding to a linear fit fairly well ($R^2 = 0.9982$), showing that the O_2 LIF signal is directly proportional to the ozone concentration. The error bars indicate the standard deviation associated with the fluctuations of the detected fluorescence signal. The laser fluence was 1.6 J/cm^2 during these measurements.

A power dependence of the signal was also carried out. The laser pulse intensity was varied by using an attenuator based on two rotatable mirrors with angle-dependent reflectivity. The slope of the power dependence curve (not shown) is 0.46, indicating partial saturation.

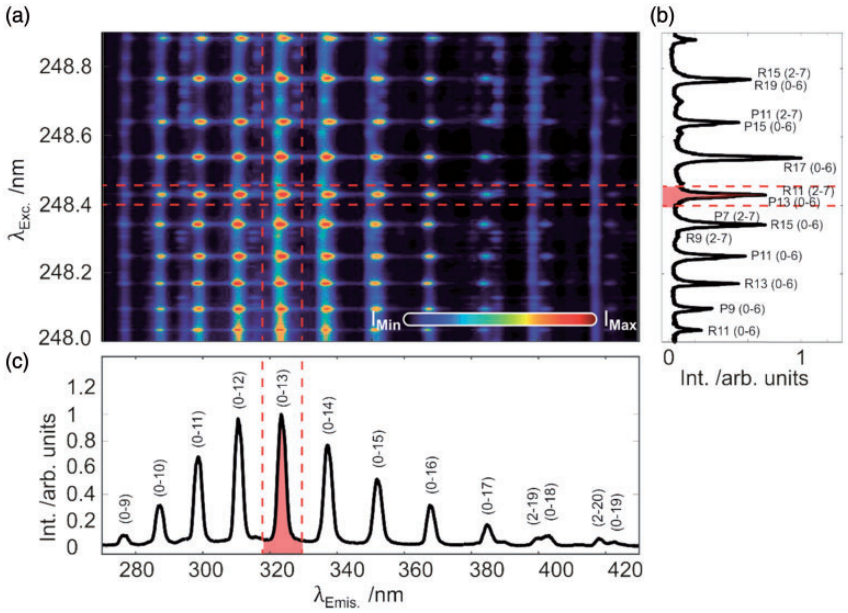

Figure 4. The recorded excitation and emission spectra of O_2 after PF-LIF of ozone presented as (a) a 2D map where (b) shows the excitation spectrum of the O_2 ($X^3\Sigma_g^-$, $v'' = 6,7$) fragments and (c) shows the emission spectrum of O_2 after excitation of the closely spaced absorption lines P(13) (0–6) and R(11) (2–7). Spectroscopic assignment of the emission and excitation features associated with the O_2 ($X^3\Sigma_g^-$, $v'' = 6,7$) fragment is presented in (b) and (c).

The slope is, however, determined both by the photolysis of ozone and the LIF process of the hot O_2 fragments. Since the laser pulse is responsible for both photodissociation and inducing fluorescence from O_2 fragments, it is not possible to obtain unambiguous information about the saturation processes, i.e., the photolysis and/or the LIF might be partially saturated. There are several advantages of being in the saturated regime, especially if imaging is considered. For example, the photolysis yield is rather high throughout the entire PLIF image and, thus, inhomogeneities in the laser sheet as well as absorption profiles will have insignificant impact on the detected signals. In addition, maximum signal intensity is obtained under saturated conditions that could, in principle, lower the detection limit even further with higher pulse energies. The slope of the power dependence curve varies within the measurement volume due to absorption and signal trapping. This issue will be discussed in the section about quantitative 2D imaging.

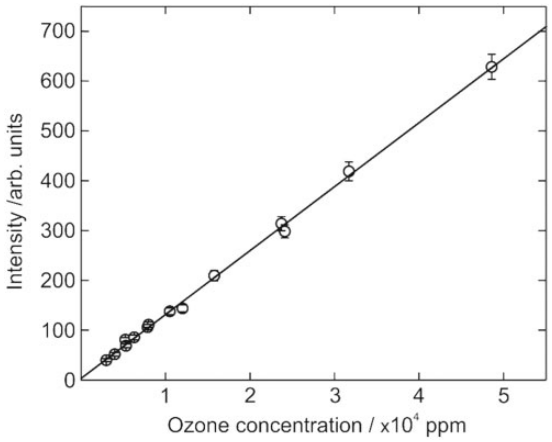

Figure 5. Concentration dependence of the O_2 fluorescence signal for different ozone concentrations.

Simultaneous Spectroscopic and Imaging Study

In this study, the O_2 fluorescence generated in a flow containing CH_4/air/O_3 was simultaneously captured with the ICCD camera and the spectrograph. The study was carried out in order to investigate how an environment containing other species than ozone and O_2 would affect quantification. For the spectrograph measurements, the emission intensity originating from a single O_2 absorption line (R(15), at 248.34 nm) was integrated, whereas for the camera measurements all emission above 249 nm (transmission edge of the filter in front of the camera) was included. Due to wavelength instability of the excimer laser, the laser was only scanned over the R(15) line. In the spectrograph study, the peak corresponding to the emission between 337.1 and 339.7 nm ($v''=14$) was integrated while all emission lines were captured with the ICCD camera. The results are presented in Figure 6, where Figure 6a shows a 2D representation of the emission spectrum while scanning the laser across the R(15) line. Each row represents a scanning step and each scanning step is a vertical integration over the signal in the raw

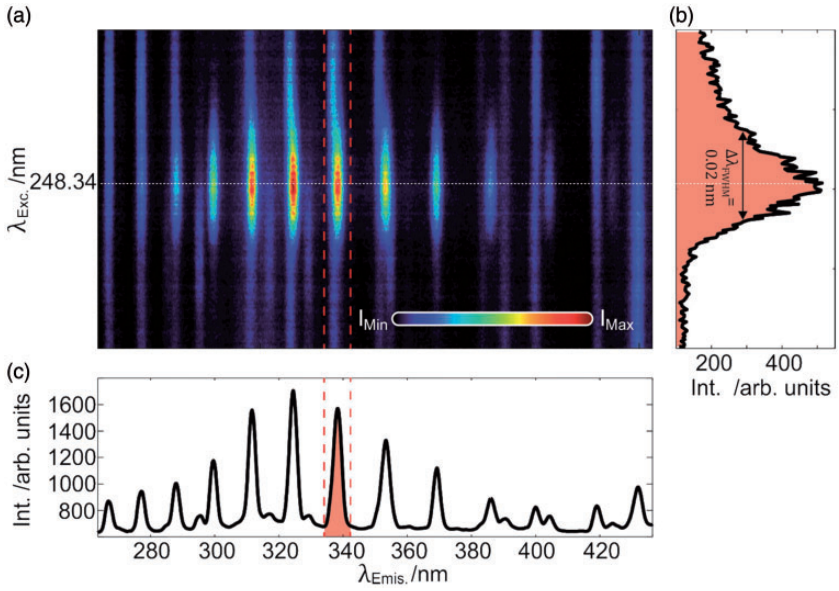

Figure 6. Spectroscopic investigation of potential interfering species in a gas mixture of CH_4/air/O_3. A 2D emission spectrum (a) over the R(15) absorption line is presented where the (b) R(15) line is shown as the vertical cross-section of the red dashed box in (a) and (c) is the horizontal cross-section of the O_2 emission of the R(15) line at 248.34 nm. The red filled peak is the $v''=14$ emission line in the range of 337.1–339.7 nm.

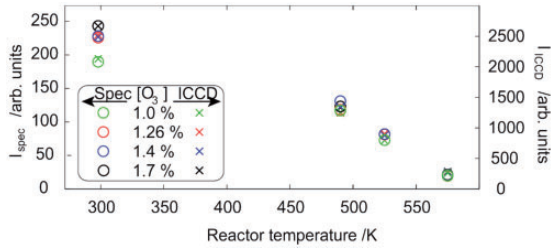

Figure 7. Simultaneous measurements of O_2 fluorescence captured with either an ICCD camera (crosses) or a spectrograph (circles). The good agreement between the spectrograph study and the ICCD measurement indicates that the emission captured on the ICCD camera is originating from O_2 emission.

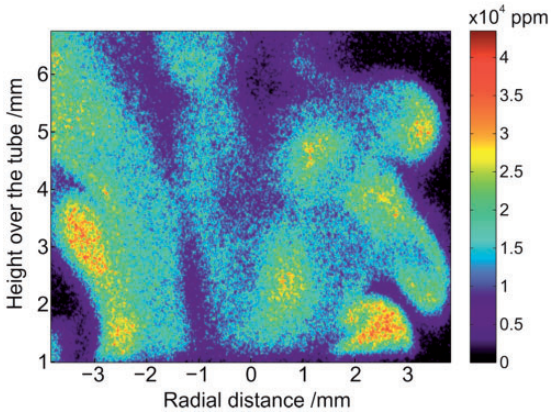

Figure 8. Quantitative turbulent single shot 2D measurements of ozone using PF-LIF. The color bar shows the ozone concentration in ppm.

data image. Figure 6b displays the intensity variation of the O_2 emission along the $v''=14$ emission line during the scan, indicated in the red dashed box in Figure 6a. There is a slight asymmetry in the curve shown in Figure 6b, which is due to an overlapping transition from the P(7) absorption line at 248.37 nm. Figure 6c shows the O_2 emission spectrum of the R(15) line, indicated by the horizontal white dashed line. Here, the $v''=14$ line is indicated as the filled red peak. Despite the fact that the measurement volume does not only contain O_3 but also various species created from the CH_4/air/O_3 flow, such as OH and CH_2O, the emission spectrum shown in Figure 6c agrees rather well with the emission spectrum presented in Figure 4c. The influence from the species in the measurement volume will be discussed below.

In Figure 7 the temperature of the reactor has been increased which causes more ozone to thermally decompose, resulting in decreasing signal strength. Here, the open circles designate the spectrograph data, while the crosses correspond to the imaging data collected with the ICCD camera. The spectrograph and imaging data were recorded simultaneously. There is a good agreement between the crosses and circles, which indicates that all captured emission by the camera is originating from O_2. The gas flow contains CH_4 and subsequent chemical reactions create various hydrogen compounds, which has been described in detail by Weng et al.[31] Despite this variety of species in the measurement volume, their potential emission contribution on the ICCD camera is insignificant compared to the O_2 signal stemming from ozone. Accurate ozone concentration may thus be extracted using a camera only.

Quantitative Two-Dimensional Measurements

Quantitative 2D imaging of ozone was demonstrated in a turbulent ozone flow containing ~3% ozone using a laser fluence of 1.1 J/cm^2. A typical single-shot image is presented in Figure 8. The image has been calibrated using known mixtures of O_3 as presented in Figure 5 and the imaging data have been corrected for differences in laser fluence by using an average power dependence value. In addition, the evaluated ozone concentration is calibrated so that each pixel has a specific calibration factor. Assuming that the laser beam profile in the single-shot case is similar to the calibration case, then this correction compensates for any inhomogeneities in the laser beam profile. A 15% shot-to-shot fluctuation in laser fluence (rms) was determined by monitoring the pulse energy of the excimer laser. These fluctuations cause a 3% uncertainty in the evaluated ozone concentration. Further, due to different flow volumes for the turbulent and the homogeneous calibration case, the effect of trapping of the LIF signal will vary, which will increase the uncertainty. The spatial resolution is limited by the thickness of the laser sheet, which is roughly 600 μm, and the imaging optics, 0.02 mm/pixel in both the horizontal and vertical direction, giving a resolution of $0.02 \times 0.02 \times 0.6\,\text{mm}^3$ for the 2D measurements. The detection limit has been estimated to ~400 ppm for single-shot measurements. The LIF process is rather saturated and increasing the pulse energy will therefore not affect the detection limit significantly. The sensitivity may be improved further if a camera with higher quantum efficiency as well as a lens with lower *f*-number is used in front of the camera.

The excitation scheme of this measurement approach involves two steps where collisional quenching could be a potential loss factor after photodissociation of ozone as well as after electronic excitation of O_2. Detailed studies of vibrational energy transfer rates in O_2, carried out by Ahn,[32] show that such processes occur at a much longer timescale than the pulse duration of the excimer laser (~17 ns). However, collisionally induced vibrational energy transfer dynamics could be problematic at higher pressures where the collisional frequency increases. In principle, this could be circumvented by using ultra-short pulse durations in the picosecond regime. Further, the dominating loss factor for electronically excited O_2 is predissociation,

which has a rate of less than 100 ps.[33] Hence, the effect of collisional quenching on vibrationally excited O_2 molecules in $v''=6$ and electronically excited O_2 (in the $B^3\Sigma_u^-$ state) is insignificant.

Potential Applications

The authors believe that this measurement technique has most potential in environments where the O_3 concentration is in the order of 500 ppm or higher. Examples of such environments may be sterilization of food packages, where either O_3 acts as sterilization agent or is an undesired byproduct in e-beam treatment, remediation of water and soil, and plasma-assisted combustion.

High temperature and non-equilibrium environments may, however, contain unwanted interfering species that also may be excited by the 248 nm laser pulse. Except for excitation of the vibrationally hot O_2 fragments, the scanning range of the KrF excimer laser does also cover OH A–X (0,3),[34] NO A–X (0,2),[35] H_2O (two-photon),[25] and naturally present vibrationally hot O_2 absorption lines. The emission from two-photon excitation of H_2O is in the range of 400–500 nm,[25] wherefore any potential signal contribution from H_2O may be suppressed by using a shortpass filter. OH excitation in the scanning range of the excimer laser as well as the subsequent fluorescence lines can be seen in Andresen et al.[30] Selecting an excitation wavelength for O_2 that does not overlap with an OH absorption line will suppress any potential undesired interfering signal contribution from OH. In addition, a band pass filter in front of the detection system aiming to suppress the OH emission could be used to suppress any undesired signal contribution even further. Moreover, NO excitation via the A–X (0,2) transition has a band head at approximately 247.95 nm,[35] wherefore tuning the excimer laser to a longer wavelength will suppress any potential interfering signal from NO. To distinguish between naturally present vibrationally hot O_2 and the created vibrationally hot O_2 photofragments a measurement concept based on PF-LIF and structured illumination may be used.[36] This is a pump-probe concept where the photolysis and the probe pulse are assigned two different laser wavelengths. Moreover, the photolysis laser beam is periodically spatially modulated, resulting in a modulated fluorescence signal from which the O_2 fragment LIF signal can be distinguished with a properly selected time delay between the pulses. In addition, initial studies of ozone, using the presented measurement concept, in a gliding arc discharge have shown that the lifetime of the vibrationally hot O_2 is much shorter than the lifetime of ozone in the gliding arc discharge. Thus, it may be possible to distinguish between the naturally present vibrationally hot O_2 and the created O_2 photofragments by utilizing the difference in lifetime of the detected laser-induced signals. By carefully considering all potential interfering species present in the measurement volume and selecting both excitation wavelength and filter in front of the detection system, quantitative O_3 imaging may be achieved in different kinds of chemical environments.

Conclusion

Quantitative imaging of ozone based on PF-LIF using a KrF excimer laser at 248 nm has been presented in this paper. In this concept, the O_3 molecule is first dissociated into O_2 and O photofragments by the 248 nm laser pulse, whereupon the same laser pulse excites the vibrationally hot O_2 photofragment that emits fluorescence upon de-excitation. The 2D measurements were demonstrated in a turbulent flow of ozone gas surrounded by ambient air. The quantification was carried out through calibration measurements of the O_2 fluorescence signal in known mixtures of ozone. The features of the detected fluorescence signal stemming from vibrationally hot O_2 were characterized in terms of both emission and absorption and any possible interference from OH, NO, and H_2O can be taken care of by considering proper wavelength selection for both excitation and detection of emission. Additional simultaneous measurements using an ICCD camera and a spectrograph were carried out to investigate if other species would influence the O_2 emission intensity. It was found that the emission contribution from a flow of CH_4/air/O_3 was negligible compared to the strong O_2 LIF signal, thus proving the capacity of quantitative ozone imaging using an ICCD camera. The authors believe that the technique has its strongest merits in environments where the ozone concentration is 500 ppm or higher, for example in plasma-assisted combustion studies and sterilization of food packages.

Acknowledgments

The authors thank Tetra Pak Packaging Solutions and O3-Technology AB for their important input.

Conflict of Interest

The authors report there are no conflicts of interest.

Funding

The authors thank the Swedish Energy Agency (Energimyndigheten) and the European Research Council (ERC) (through the advance grant TUCLA) for their financial support.

References

1. J.H. Seinfeld, S.N. Pandis. "Atmospheric Trace Constituents". *In:* Atmospheric Chemistry and Physics: From Air Pollution to Climate Change, 2nd ed., Chap. 2. Hoboken, NJ: John Wiley and Sons, 2006, pp.52–55.
2. K.Y. Kondratyev, C. Varotsos. "Remote Sensing and Global Tropospheric Ozone Observed Dynamics". Int. J. Remote Sens. 2002. 23(1): 159–178.
3. A. Ehn, J.J. Zhu, P. Petersson, Z.S. Li, M. Aldén, C. Fureby, T. Hurtig, N. Zettervall, A. Larsson, J. Larfeldt. "Plasma Assisted Combustion: Effects of O_3 on Large Scale Turbulent Combustion Studied with

Laser Diagnostics and Large Eddy Simulations". Proc. Combust. Inst. 2015. 35(3): 3487–3495.
4. T. Ombrello, S.H. Won, Y. Ju, S. Williams. "Flame Propagation Enhancement by Plasma Excitation of Oxygen. Part I: Effects of O_3". Combust. Flame. 2010. 157(10): 1906–1915.
5. Z.H. Wang, L. Yang, B. Li, Z.S. Li, Z.W. Sun, M. Aldén, K.F. Cen, A.A. Konnov. "Investigation of Combustion Enhancement by Ozone Additive in CH4/Air Flames Using Direct Laminar Burning Velocity Measurements and Kinetic Simulations". Combust. Flame. 2012. 159(1): 120–129.
6. X. Liang, Z. Wang, W. Weng, Z. Zhou, Z. Huang, J. Zhou, K. Cen. "Study of Ozone-Enhanced Combustion in H2/CO/N2/Air Premixed Flames by Laminar Burning Velocity Measurements and Kinetic Modeling". Int. J. Hydrogen Energy. 2013. 38(2): 1177–1188.
7. S. Patil, T. Moiseev, N.N. Misra, P.J. Cullen, J.P. Mosnier, K.M. Keener, P. Bourke. "Influence of High Voltage Atmospheric Cold Plasma Process Parameters and Role of Relative Humidity on Inactivation of Bacillus Atrophaeus Spores Inside A Sealed Package". J. Hosp. Infect. 2014. 88(3): 162–169.
8. M. Laroussi. "Low Temperature Plasma-Based Sterilization: Overview and State-Of-The-Art". Plasma Process Polym. 2005. 2(5): 391–400.
9. M. Moisan, J. Barbeau, S. Moreau, J. Pelletier, M. Tabrizian, L. Yahia. "Low-Temperature Sterilization Using Gas Plasmas: A Review of the Experiments and an Analysis of the Inactivation Mechanisms". Int. J. Pharm. 2001. 226(1-2): 1–21.
10. V. Scholtz, J. Pazlarova, H. Souskova, J. Khun, J. Julak. "Nonthermal Plasma—A Tool for Decontamination and Disinfection". Biotechnol. Adv. 2015. 33(6): 1108–1119.
11. M.R. Pervez, A. Begum, M. Laroussi. "Plasma Based Sterilization: Overview and the Stepwise Inactivation Process of Microbial by Non-Thermal Atmospheric Pressure Plasma Jet". Int. J. Eng. Technol. 2014. 14(5): 7–16.
12. J. Ehlbeck, U. Schnabel, M. Polak, J. Winter, T. Von Woedtke, R. Brandenburg, T. Von Dem Hagen, K.-D. Weltmann. "Low Temperature Atmospheric Pressure Plasma Sources for Microbial". J. Phys. D: Appl. Phys. 2011. 44(1): 013002.
13. S.J. Masten, S.H.R. Davies. "Efficacy of In-Situ Ozonation for the Remediation of PAH Contaminated Soils". J. Contam. Hydrol. 1997. 28(4): 327–335.
14. J. Rivas, O. Gimeno, R.G. De La Calle, F.J. Beltrán. "Ozone Treatment of PAH Contaminated Soils: Operating Variables Effect". J. Hazard. Mater. 2009. 169(1-3): 509–515.
15. O.G. Apul, P. Dahlen, A.G. Delgado, F. Sharif, P. Westerhoff. "Treatment of Heavy, Long-Chain Petroleum-Hydrocarbon Impacted Soils Using Chemical Oxidation". J. Environ. Eng. 2016. 142(12): 04016065–1. doi: 10.1061/(ASCE)EE.1943-7870.0001139.
16. N. Lu, C. Wang, C. Lou. "Remediation of PAH-Contaminated Soil by Pulsed Corona Discharge Plasma". J. Soils Sediments. 2017. 17(1): 97–105.
17. M. Mehrjouei, S. Müller, D. Möller. "A Review on Photocatalytic Ozonation Used for the Treatment of Water and Wastewater". Chem. Eng. J. 2015. 263: 209–219.
18. P. Mondal, S. Bhowmick, D. Chatterjee, A. Figoli, B. Van Der Bruggen. "Remediation of Inorganic Arsenic in Groundwater for Safe Water Supply: A Critical Assessment of Technological Solutions". Chemosphere. 2013. 92(2): 157–170.
19. R. Ono, T. Oda. "Dynamics of Ozone and OH Radicals Generated by Pulsed Corona Discharge in Humid-Air Flow Reactor Measured by Laser Spectroscopy". J. Appl. Phys. 2003. 93(10): 5876–5882.
20. K. Kohse-Höinghaus. "Laser Techniques for the Quantitative Detection of Reactive Intermediates in Combustion Systems". Prog. Energy Combust. Sci. 1994. 20(3): 203–279.
21. J.W. Daily. "Laser Induced Fluorescence Spectroscopy in Flames". Prog. Energy Combust. Sci. 1997. 23(2): 133–199.
22. M. Aldén, J. Bood, Z. Li, M. Richter. "Visualization and Understanding of Combustion Processes Using Spatially and Temporally Resolved Laser Diagnostic Techniques". Proc. Combust. Inst. 2011. 33(1): 69–97.
23. Y. Matsumi, M. Kawasaki. "Photolysis of Atmospheric Ozone in the Ultraviolet Region". Chem. Rev. 2003. 103(12): 4767–4782.
24. O. Johansson, J. Bood, M. Aldén, U. Lindblad. "Detection of Hydrogen Peroxide Using Photofragmentation Laser-Induced Fluorescence". Appl. Spectrosc. 2008. 62(1): 66–72.
25. K. Larsson, O. Johansson, M. Aldén, J. Bood. "Simultaneous Visualization of Water and Hydrogen Peroxide Vapor Using Two-Photon Laser-Induced Fluorescence and Photofragmentation Laser-Induced Fluorescence". Appl. Spectrosc. 2014. 68(12): 1333–1341.
26. O. Johansson, J. Bood, B. Li, A. Ehn, Z.S. Li, Z.W. Sun, M. Jonsson, A.A. Konnov, M. Aldén. "Photofragmentation Laser-Induced Fluorescence Imaging in Premixed Flames". Combust. Flame. 2011. 158(10): 1908–1919.
27. B. Li, M. Jonsson, M. Algotsson, J. Bood, Z.S. Li, O. Johansson, M. Aldén, M. Tunér, B. Johansson. "Quantitative Detection of Hydrogen Peroxide in an HCCI Engine Using Photofragmentation Laser-Induced Fluorescence". Proc. Combust. Inst. 2013. 34(2): 3573–3581.
28. R.W. Pitz, T.M. Brown, S.P. Nandula, P.A. Skaggs, P.A. Debarber, M.S. Brown, J. Segall. "Unseeded Velocity Measurement by Ozone Tagging Velocimetry". Opt. Lett. 1996. 21(10): 755–757.
29. J.H. Grinstead, G. Laufer, J.C. Mcdaniel. "Single-Pulse, Two-Line Temperature-Measurment Technique Using KrF Laser-Induced O_2 Fluorescence". Appl. Opt. 1995. 34(24): 5501–5512.
30. P. Andresen, A. Bath, W. Gröger, W. Lülf, G. Meijer, J.J. Meulen. "Laser-Induced Fluorescence with Tunable Excimer Lasers as a Possible Method for Instantaneous Temperature Field Measurements At High Pressures: Checks with an Atmospheric Flame". Appl. Opt. 1988. 27(2): 365–378.
31. W. Weng, E. Nilsson, A. Ehn, J. Zhu, Y. Zhou, Z. Wang, Z. Li, M. Aldén, K. Cen. "Investigation of Formaldehyde Enhancement by Ozone Addition in CH4/Air Premixed Flames". Combust. Flame. 2015. 162(4): 1284–1293.
32. T.S. Ahn. Determination of Vibration-To-Vibration Energy Transfer Rates of Nitrogen, Oxygen, and Hydrogen Using Stimulated Raman Scattering. [Doctor of Philosophy Dissertation]. Columbus, OH: Ohio State University, 2005.
33. M.J. Daniels, J.R. Wiesenfeld. "Rotational Population Distributions of O2(X v''=9, 12, and 15) Following Ozone Photolysis at 248 nm". J. Chem. Phys. 1993. 98(1): 321–330.
34. W. Ketterle, M. Schäfer, A. Arnold, J. Wolfrum. "2D Single-Shot Imaging of OH Radicals Using Tunable Excimer Lasers". Appl. Phys. B. 1992. 54(2): 109–112.
35. C. Schulz, B. Yip, V. Sick, J. Wolfrum. "A Laser-Induced Fluorescence Scheme for Imaging Nitric Oxide in Engines". Chem. Phys. Lett. 1995. 242(3): 259–264.
36. K. Larsson, M. Jonsson, J. Borggren, E. Kristensson, A. Ehn, M. Aldén, J. Bood. "Single-Shot Photofragment Imaging by Structured Illumination". Opt. Lett. 2015. 40(21): 5019–5022.